# Complete electromagnetically induced transparency in sodium atoms excited by a multimode dye laser

G. Alzetta, S. Gozzini,* and A. Lucchesini
*IPCF-CNR, Area della Ricerca, Via G. Moruzzi 1, 56124 Pisa, Italy*

S. Cartaleva and T. Karaulanov
*Institute of Electronics, BAS, boul. Tzarigradsko shosse 72, 1784 Sofia, Bulgaria*

C. Marinelli and L. Moi
*INFM-Università di Siena, Dipartimento di Fisica, Via Roma 56, 53100 Siena, Italy*
(Received 7 October 2003; revised manuscript received 1 March 2004; published 22 June 2004)

Complete electromagnetically induced transparency (EIT) in sodium vapor is demonstrated experimentally by means of excitation with a broadband multimode dye laser tuned on the $D_1$ line. One hundred percent transparency is observed by excitation of the Na vapor with circularly polarized laser light. The linear polarization excitation produces, instead, complete destruction of the EIT resonance. For laser power density in the 0.1 to 1 $W/cm^2$ range, the linewidth of the EIT resonance remains in the interval of 90–400 kHz. This complete transparency of the medium in a narrow frequency interval is interesting for many applications where the enhancement of the refractive index is important and where the improvement of the signal-to-noise ratio of the dark resonances allows a more sensitive measurement of weak magnetic fields.

DOI: 10.1103/PhysRevA.69.063815 PACS number(s): 42.50.Gy, 32.80.−t

## I. INTRODUCTION

Coherent excitation of ground-state atoms results in interesting effects that open important perspectives in fundamental physics and applications. Among others, coherent population trapping (CPT) and the related effect of electromagnetically induced transparency (EIT) are nowadays extensively studied and applied to fields as different as laser cooling of atoms [1], precise magnetic field measurements [2], atomic clocks [3], slowing down of light [4] and others.

CPT manifests itself as a fluorescence quenching transition with linewidth orders of magnitude narrower than the natural width of the corresponding optical transitions. CPT resonances have been studied in many alkali atoms: in particular, three-level $\Lambda$ systems involving either one [5] or both [6] ground state hf levels $F_g$ have been studied in sodium. In the first case, a properly polarized monochromatic laser field is sufficient to induce the CPT resonance due to the fact that different polarization components connect couples of degenerate ground state Zeeman sublevels to a common excited state. These resonances, that we denote as magnetic coherence (MC) resonances, are excited at zero magnetic field and are detected by scanning it around its zero value.

Main problems for full understanding of the effect arise from the complex level structure of the atoms, as the two or three level atom models are crude simplifications of the effective atomic level structure. In fact differences among the results expected from the model and the results obtained in the experiments are usually observed: this makes useful a detailed analysis with a model taking into account the effective level structure of the atom. Among other competing effects, optical pumping is very important as it accumulates the atomic population into levels not involved in the laser excitation. In fact, a dramatic decrease of the MC resonance contrast is observed that may reach the value of 50% as shown in previous experiments [5,7]. A strong and steep resonant enhancement of the refractive index can be observed only in the case of vanishing absorption of atomic medium. In order to achieve this, Rb atoms have been excited by means of three lasers with controlled frequency [8]. The refractive index enhancement is the main cause of the significant slowing down of the group velocity of light [9].

In this paper we propose a simple method to make the population losses negligible by involving all atoms of the Na ground state in the formation of the narrow coherent resonances. The basic idea for overcoming the loss during the MC resonance preparation is to excite the $D_1$ line with a multimode dye laser, whose spectral bandwidth is larger than the $D_1$ absorption linewidth and whose longitudinal mode separation is comparable with the natural linewidth. This inhibits hf optical pumping. Moreover, when a large number of laser modes is used, all velocity classes of the Na atoms are resonant with the radiation and contribute to the MC resonance, with automatic compensation for the loss due to velocity-changing collisions.

Another advantage given by this approach is that the total laser power is spread over a large number of modes, each interacting with different atoms. This reduces the power broadening effect and makes all atoms exhibiting narrow fluorescence resonances at zero magnetic field. As a result, dark resonances with a contrast up to 100% and a significant decrease in the resonance linewidth have been observed. They are detected looking at the atomic fluorescence when the applied magnetic field is scanned around its zero value.

*Electronic address: silvia@ipcf.cnr.it

 

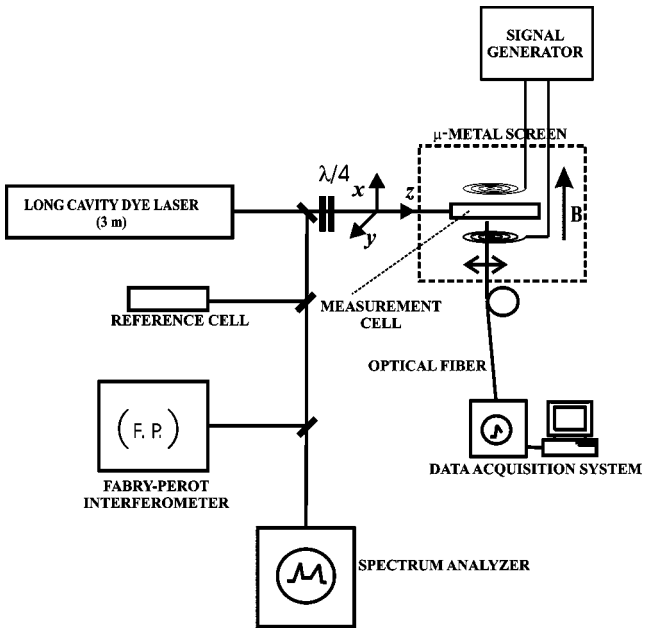


FIG. 1. Experimental setup.

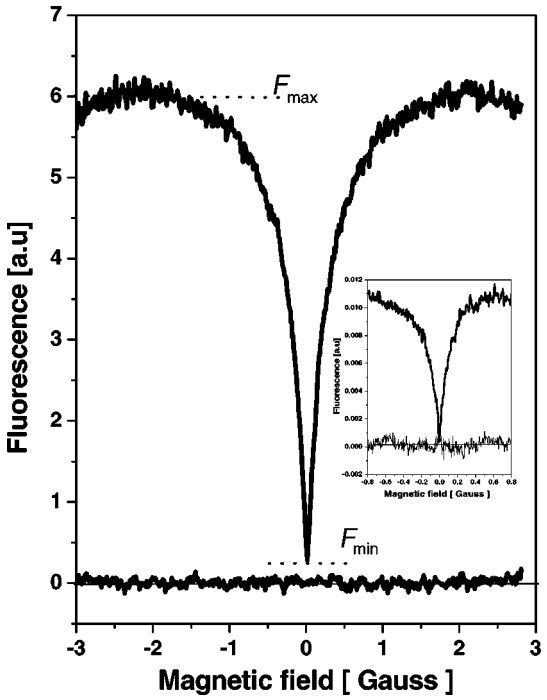


FIG. 2. Example of dark MC resonance obtained by sweeping B around its zero value. The zero line is obtained by detuning the laser out of resonance. The fluorescence levels used to determine the contrast C are shown. In the inset approaching of the complete transparency is shown for the coated cell: $I_L = 360$ mW/cm$^2$, $T = 103$ °C.

Results are obtained with two different experimental configurations that use either linearly polarized or circularly polarized laser light. These different polarizations lead to different population redistribution among Zeeman and hf levels and, because of that, to different results. In this paper we present the experimental results obtained together with a theoretical analysis according to a multilevel rate equation scheme.

## II. EXPERIMENTAL SETUP

The experimental setup is shown in Fig. 1. As already discussed, the main idea is to use a broadband laser able to excite at the same time all atoms in the ground state independently of their velocity or of their sublevel occupation. Thus, we follow a very simple approach which has been successfully used in Hanle effect and optical pumping experiments [10,11]. There are many possible ways to generate such a spectrum. The main tool is a free running multimode laser having a cavity adjusted in length in order to fit the experiment requirements [12]. Suitable etalons have been inserted in the cavity to tailor the spectrum profile and optimize the laser-vapor coupling. A dye laser with cavity length variable between 0.5 m to more than 3 m is tuned to the $D_1$ line of sodium. When the cavity is short, three stable modes can be selected with 1705 MHz frequency difference. Increasing the cavity length up to 3 m, a dense spectrum of longitudinal modes separated by 50 MHz is obtained which covers a frequency interval of about 5 GHz. In this way we obtain about 40 modes resonant with the vapor within the Doppler profile; this induces transitions from both the hyperfine sublevels of the ground states. This particular configuration has been successfully applied in experiments in which a huge vapor-radiation coupling is required (see, for example, [13]). The distance between the laser modes is measured by means of the beat signals detected by a fast photodiode connected to a spectrum analyzer. The laser spectrum is controlled also by means of a Fabry-Perot interferometer with 8 GHz FSR. The diameter of the laser beam falling on the cell is 6 mm. The sodium vapor is confined in Pyrex cells having different characteristics. The experiments have been performed with a cell containing only Na vapor (noted as vacuum cell), with a poly-dimethyl-siloxane (PDMS) coated vacuum cell (coated cell) and with a cell filled with 6 Torr of Ar (buffer gas cell). The coating has the property to preserve the atomic orientation or alignment in the collisions with the walls. The laboratory magnetic field has been shielded by means of a $\mu$-metal cylinder, in which a solenoid or a couple of Helmholtz coils are inserted. They in turn generate a magnetic field that is modulated around the zero value. The solenoid is oriented parallel and the Helmholtz coils perpendicular to the laser beam, respectively. The atomic fluorescence is collected by a fiber at right angle with respect to the laser beam propagation direction, and measured in dependence on magnetic field. In some experiments (see [14] and references therein) this kind of resonance is registered as magneto-optical rotation of the probe beam polarization.

In Fig. 2 an example of a MC signal is presented which is obtained in the transverse field configuration with long cavity laser. From the fluorescence intensity variation at the occurrence of the coherence, we extract the value of the contrast, defined in our case as

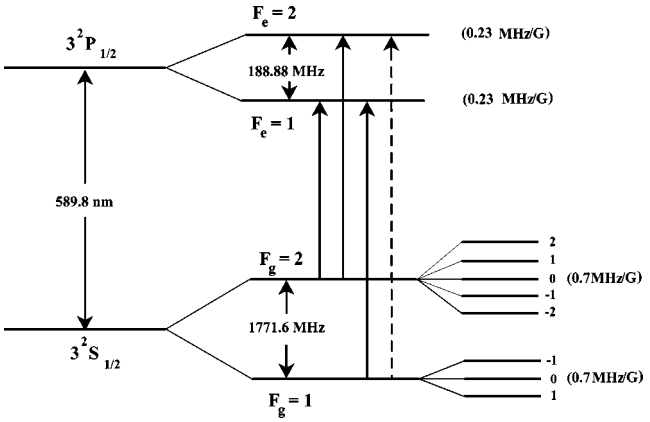


FIG. 3. The hf level structure of the $D_1$ sodium line. The frequency separation between the hf levels is reported and the Zeeman splitting per Gauss between adjacent magnetic sublevels is given. Two different kinds of transitions are distinguished: $F_g \rightarrow F_e = F_g$, $F_g - 1$ (solid line), and $F_g \rightarrow F_e = F_g + 1$ (dashed line).

$$C = (\mathcal{F}_{\max} - \mathcal{F}_{\min})/\mathcal{F}_{\max}, \tag{1}$$

where $\mathcal{F}_{\max}$ and $\mathcal{F}_{\min}$ are the fluorescence levels out of and in the MC resonance. In the figure insert, the 100% contrast is shown for the PDMS coated cell.

## III. MC RESONANCES EXCITATION SCHEME AND EXPERIMENTAL RESULTS

The hf levels and transitions of the sodium $D_1$ line are sketched in Fig. 3.

The Doppler width of the hf transitions at 400 K is about 1.53 GHz and the natural width is 9.9 MHz [15]. As the frequency difference of the two ground-state hf levels is $\Delta\nu_{\rm hf} = 1771.6$ MHz, the hf transitions have considerable overlapping of the Doppler profiles. The hf transitions according to the $F$ value of the involved levels are denoted in Fig. 3 by dashed or solid lines. When depolarizing collisions or population losses can be neglected, the $F_g \rightarrow F_e = F_g$, $F_g - 1$ transitions lead to the observation of EIT MC resonances [5], while the $F_g \rightarrow F_e = F_g + 1$ transitions lead to electromagnetically-induced absorption (EIA, or bright) MC resonances [16]. An additional condition for the bright resonance observation is the population loss to the ground state hf level not interacting with the laser field to be less than 50% [17,18]. MC resonances can be observed with different relative orientations of laser polarization E, direction of beam propagation $k$, and magnetic field direction B. In [19] it has been shown that the measured variation of the fluorescence with the magnetic field is of the same sign (dark or bright resonance) for excitation with linearly polarized light and B parallel to $k$, as for the case of circular polarization of the laser beam and B perpendicular to $k$. The two cases will be discussed here in more detail, taking as an example the $F_g = 2 \rightarrow F_e = 2$ transition. For both of them, the quantization axes are chosen in a way to make the description and the calculations in Sec. IV easier and more intuitive. The MC resonance sign reversal will be discussed for the $F_g = 1 \rightarrow F_e = 2$ transition. Two sets of experiments have been made.

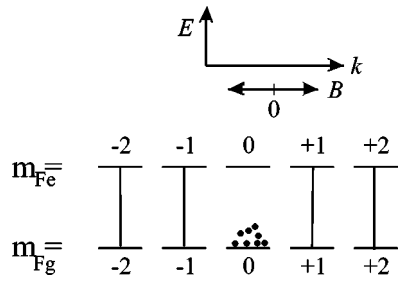


FIG. 4. Population distribution among Zeeman sublevels in case of linear polarization of the light in the $F_g = 2 \rightarrow F_e = 2$ transition.

In the first set, the magnetic field is collinear to the propagation direction of the laser field $k$ ($z$ direction in Fig. 1) whose polarization is linear (electric vector E in $x$ direction). In the second set of experiments Na atoms were irradiated by a circularly polarized laser beam propagating along the $z$ direction, while the magnetic field in the $y$ direction was applied and scanned around $B_y = 0$.

### A. Linear polarization of the laser light and B parallel to *k*

As the dark resonance is observed in a narrow interval of the magnetic field around $B = 0$, the direction of E is taken as a quantization axis (Fig. 4).

At $B = 0$, $\pi$ transitions produce optical pumping to the $m_{F_g} = 0$ Zeeman sublevel which is not excited by the laser field. In this way the alignment of the angular momentum of the atoms and the minimum of the fluorescence occur. When a small B along the laser beam is applied, the fluorescence increases due to the magnetic transitions between ground-state Zeeman sublevels. Thus, dark resonance in the fluorescence in dependence on the magnetic field is observed with subnatural width determined mainly by the width of the ground-state sublevels [15,20].

According to previous works [5,21], where a population loss reduction gave a resonance contrast increment, we expected a similar result in our case, i.e., a strong enhancement of the resonance contrast following the broadening of the laser spectrum. We have attempted to see MC resonances in our different cells, but MC dark resonance centered at $B_z = 0$ has been observed only in the vacuum cell. For this cell a detailed analysis as a function of the laser spectrum has then been made. MC resonance with a maximum contrast of the order of 30% was observed using a three-mode laser spectrum, while no signal has been observed by increasing the number of modes and the spectral bandwidth of the laser field.

As shown in [5], in the case of Na atomic beam irradiated by linear-polarization single-frequency laser beam, dark resonances have been observed for all transitions with $F_g \rightarrow F_e = F_g, F_g - 1$, while no narrow lines have been observed for $F_g \rightarrow F_e = F_g + 1$ transitions. In that experiment, the laser field excites only one hf transition. Instead, in the case of Na atoms confined in a cell, the single-mode laser field excites more than one hf transition due to the Doppler broadening. For a three-mode laser, different velocity classes are excited for different hf transitions. In this way each atom "sees" only

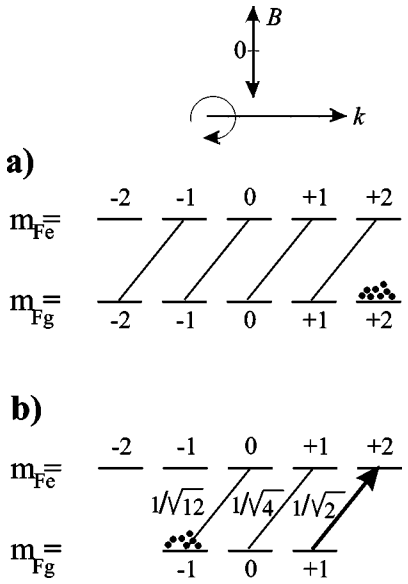


FIG. 5. Population distribution among Zeeman sublevels upon $\sigma^+$ excitation for the transitions $F_g=2\rightarrow F_e=2$ (a) and $F_g=1\rightarrow F_e=2$ (b).

one laser mode at a time and the excitations can be considered independent. When instead the number of modes is strongly increased, the same atoms could interact with many of them, inducing all possible hf transitions of the $D_1$ line. The consequence is that the excitation of a given hf transition is not independent of the other excited hf transitions. This produces, as will be demonstrated in Sec. IV, the equalization of the population on all ground-state Zeeman sublevels and the resonance inhibition.

### B. Circular polarization of the light and B perpendicular to *k*

If the sample is irradiated with circularly polarized light, the Zeeman optical pumping of the atoms to the $m_{F_g}=+2$ level, hence, orientation along $k$, takes place at $B=0$. This determines a minimum in the fluorescence [Fig. 5(a)]. When a small $B\perp k$ is applied, this will result in a redistribution of population among the ground-state Zeeman sublevels and in an increase of the fluorescence. Consequently, a dark resonance is observed.

When several Torrs of buffer gas are added to the cell, some mixing of population between the excited-state Zeeman sublevels will take place due to collisions between Na and buffer gas atoms. The excited state depolarizing collisions do not influence critically the MC resonances involving $F_g\rightarrow F_e=F_g$, $F_g-1$ transitions. They are instead responsible for a reversal of the resonance in the case of $F_g\rightarrow F_e=F_g+1$ transitions, as observed in Cs [22].

Let us consider the $F_g=1\rightarrow F_e=2$ transition in Na. In the absence of depolarizing collisions and in the presence of intense circularly polarized light ($\sigma^+$), most atoms will circulate in the $m_{F_g}=1\rightarrow m_{F_e}=2$ transition, that is the transition with the highest probability [Fig. 5(b)]. Because of this, a maximum in the fluorescence is observed at $B=0$. When a magnetic field perpendicular to the atomic orientation is applied, part of the population of the $m_{F_g}=1$ sublevel will be redistributed to the other sublevels and the fluorescence will decrease. The net result is a bright resonance observation in the fluorescence versus the magnetic field. When a buffer gas is added, a fraction of the atoms accumulated on the $m_{F_e}=2$ sublevel will be redistributed among the other Zeeman sublevels ought to the depolarizing collisions. At $B=0$, taking into account the transition rate differences between the different Zeeman sublevels, this redistribution will lead to the accumulation of many atoms on the $m_{F_g}=-1$ sublevel. This has, in fact, the lowest transition probability for $\sigma^+$ excitation. Thus, the bright resonance observed in pure Na vapor transforms into a dark one when buffer gas is added to the cell. As a conclusion of the above discussion it should be pointed out that in the buffered cell all hf transitions will contribute to MC dark resonance only.

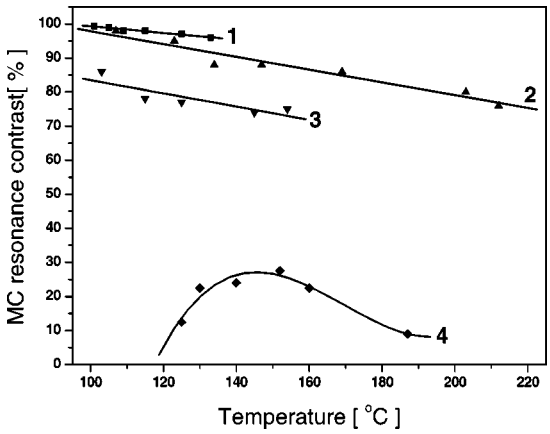


FIG. 6. MC resonances contrast C as a function of temperature. Experimental results with multimode laser for coated (1), buffer gas (2) and vacuum (3) cells. Curve (4) represents the results for three-mode laser operation in the buffer gas cell $I_L=360$ mW/cm$^2$.

Let us now discuss the behavior of the three used cells. We report the results obtained by collecting the fluorescence along the $y$ direction and calculating from Eq. (1) the contrast of the MC resonances as a function of the laser mode number and of the cell temperature, i.e., of the vapor density.

First, the buffer gas cell was irradiated by a three-mode laser beam with frequency difference between the adjacent modes $\Delta\nu_L=1705$ MHz, which is relatively far from the hf levels frequency difference $\Delta\nu_{hf}=1771.6$ MHz to avoid preparation of resonance based on two hf levels' coherent coupling. The contrast of the dark MC resonance in dependence on the temperature is shown in Fig. 6.

It can be seen that the contrast versus the temperature exhibits a maximum of 27%. Hence, significant population losses take place in the three-mode excitation case.

By switching to the multimode long cavity laser, a situation opposite to the one corresponding to excitation by linearly polarized light is obtained. Here the contrast of the dark MC resonance increases dramatically. In Fig. 6, curve (2) presents the dark MC resonance contrast in dependence on the temperature for the buffer gas cell. It can be seen that the dark resonance contrast approaches 99% for a cell temperature of 110 °C. As it was discussed above, in this case also the $F_g=1\rightarrow F_e=2$ transition contributes to the dark reso-

nance, providing almost complete transparency of the medium.

In the case of the vacuum cell, the increment of the mode number leads also to a significant enhancement of the dark resonance contrast (Fig. 6, curve 3). However, the maximum contrast value is about 85%, which is a little bit lower than the one obtained for the buffer gas cell. This is due to the fact that, unlike in the buffer gas cell, here the $F_g=1\rightarrow F_e=2$ transition produces bright instead of dark MC resonances. The simultaneous excitation of the dark and bright resonances is therefore the reason for the lower EIT resonance contrast in the vacuum cell. Some depolarization of the ground state and hence lower resonance contrast can be attributed to atom spin change relaxation to the cell walls. This is not the case of the buffer gas cell where the number of Na atom collisions with the cell walls is strongly reduced.

Maximum contrast is observed for the coated cell, where complete transparency of the medium is achieved (Fig. 6, curve 1). Here, like for the uncoated vacuum cell, the resonance obtained from excitation of the $F_g=1\rightarrow F_e=2$ transition is bright; however, in the coated cell it does not decrease the Na atoms transparency. The main advantage when using a coated cell consists in the fact that the collisions with walls do not change the spin orientation. So the same atom is back in the laser beam many times without destruction of the orientation or alignment. And this works as an enhancement of the effective interaction time of atoms with the beam. Moreover, the coherence is also preserved during these collisions. This leads to the effect that, as it will be discussed in Sec. IV, a steady state is reached where the level $F_g=1$ is completely depleted. Consequently, for excitation by circularly polarized light, the experimental results show that it is possible to overcome the population losses by increasing the number of modes and the spectral interval of the laser field. At lower cell temperature, the Na absorption vanishes, leading to complete transparency of the medium.

For the three cells, some reduction of the contrast with the temperature has been observed due to the increasing of atomic density with temperature. The atomic vapor becomes in fact optically thicker, leading to the following effects: (i) light absorption [23], (ii) spin-exchange collisions, and (iii) radiation trapping increase.

(i) Due to the absorption enhancement, the laser light intensity along the cell decreases, causing reduction in the resonance contrast.

(ii) Spin-exchange collisions, whose rates increase with the atomic density, reduce the amplitude of the resonance due to the decay of coherence between ground-state Zeeman sublevels.

(iii) Radiation trapping enhancement with atomic density [24] causes the optical pumping rate reduction.

The MC resonance contrast dependence on temperature differs significantly, when excited by a dense and broad laser spectrum, from that of the three-mode excitation. In the second case, in fact, the contrast diminishes very rapidly, as can be seen in Fig. 6, curve 4, and reported in [25]. On the contrary, in the case of multimode excitation, when the number of atoms involved in the resonance preparation is much higher, the temperature has lower influence to the resonance contrast. Here, due to the strongly increased transparency of the medium when the dark resonance occurs, the reduction of the laser beam intensity along the cell with temperature is much weaker.

## IV. RATE EQUATION MODEL

The main conclusion from the results presented in the previous section is that there is a strong difference between the multimode linear and circular polarization excitations. In the first case, the MC resonance is completely destroyed, while in the second one the resonance contrast reaches a 100% value.

This behavior follows in a simple way if only fine structure of the atomic spectrum is considered, which has been used in the case of optical pumping with broadband spectrum light. For $J=\frac{1}{2}$ ground state, there is no accumulation of atomic population at single Zeeman sublevel when $\pi$ excitation is applied, while $\sigma$ excitation results in atomic orientation. However, as we examine MC resonances produced from both narrow and broadband excitations, it is useful to apply a model which takes into consideration the hf structure of the atomic levels. In this way more information about the dynamic of Zeeman sublevel population can be obtained. Our model describes the evolution of the population of all levels involved in the interaction scheme. Using the model of [26] we can write the closed system of 16 differential equations describing the dynamics of the atomic population:

$$\frac{dN_{F_g,m_{F_g}}}{dt}=\sum_{F_e}\left(-N_{F_g,m_{F_g}}\sum_q W_{F_g,m_{F_g}\rightarrow F_e,m_{F_e}+q}+\sum_q N_{F_e,m_{F_e}+q}W_{F_e,m_{F_e}+q\rightarrow F_g,m_{F_g}}+\sum_{k=m_{F_e}-1}^{m_{F_e}+1}N_{F_e,k}A_{F_e,k\rightarrow F_g,m_{F_g}}\right),$$

$$\frac{dN_{F_e,m_{F_e}}}{dt}=\sum_{F_g}\left(\sum_q\left(N_{F_g,m_{F_g}-q}W_{F_g,m_{F_g}-q\rightarrow F_e,m_{F_e}}-N_{F_e,m_{F_e}}W_{F_e,m_{F_e}\rightarrow F_g,m_{F_g}-q}\right)-N_{F_e,m_{F_e}}\sum_{k=m_{F_g}-1}^{m_{F_g}+1}A_{F_e,m_{F_e}\rightarrow F_g,k}\right),\tag{2}$$

where $N_{F_g,m_{F_g}}, N_{F_e,m_{F_e}}$ are the populations of the ground and excited states Zeeman sublevels at the $D_1$ line of sodium and $q=0,+1,-1$ for $\pi$, $\sigma^+$ and $\sigma^-$ polarization of the laser light, respectively. The coefficients $W$ are the induced transition rates and are given by

$$W_{F_g,m_{F_g}\to F_e,m_{F_e}} = \frac{3\lambda^3 I_L}{8\pi^2 hc} A_{F_g,m_{F_g}\to F_e,m_{F_e}} \times \int_{-\infty}^{+\infty} g_{F_g,m_{F_g}\to F_e,m_{F_e}}(\nu)\rho_L(\nu)d\nu, \quad (3)$$

where λ is the laser wavelength, $h$ is the Planck constant, $c$ is the speed of light, $I_L$ is the laser intensity expressed in $W/m^2$, and $g(\nu)$ and $\rho(\nu)$ are the atomic transition and laser light spectral profiles, respectively. The case of 5 GHz multimode laser excitation is considered first: for simplicity, we assume a flat profile of the spectrum whose width is $\gamma_L$. The absorption linewidth of the atomic medium can be ignored, as it is orders of magnitude lower than $\gamma_L$. Thus, for $W$ coefficients we derive

$$W_{F_g,m_{F_g}\to F_e,m_{F_e}} = \frac{3\lambda^3 I_L}{8\pi^2 hc}\frac{1}{\gamma_L} A_{F_g,m_{F_g}\to F_e,m_{F_e}}. \quad (4)$$

The coefficient $A_{F_g,m_{F_g}\to F_e,m_{F_e}} = \alpha^2_{F_g,m_{F_g}\to F_e,m_{F_e}}/\tau$ is the spontaneous transition rate, $\tau$ is the transition lifetime and the transfer coefficients are

$$\alpha(F_e,m_{F_e};F_g,m_{F_g};q) = (-1)^{1+I+J_e+F_e+F_g-m_e} \times \sqrt{2F_g+1}\sqrt{2F_e+1}\sqrt{2J_e+1} \times \begin{pmatrix} F_e & 1 & F_g \\ -m_e & q & m_g \end{pmatrix} \begin{Bmatrix} F_e & 1 & F_g \\ J_g & I & J_e \end{Bmatrix}, \quad (5)$$

where the parentheses and curly brackets denote $3-j$ and $6-j$ coefficients, respectively. We assume the induced transition rate to be time independent, which is valid for our case of Gaussian laser profile [27]. In our approach we do not take into account any coherence, because the spectral interval of the laser excitation is greater than the transition linewidth [28]. We neglect the residual magnetic field and any depolarizing mechanisms affecting the Zeeman states or relaxation processes other than the spontaneous emission. We solve numerically the system of differential equations with the initial condition that the population of the ground state is equally distributed among its hf levels, so the population of each magnetic sublevel of the $F_g=1$ is $\frac{1}{6}$ and for $F_g=2$ it is $\frac{1}{10}$.

In the case of $\pi$ excitation (linear polarization of the light and quantization axis along the polarization vector), our calculations show that the laser field does not induce any accumulation of population on a particular ground-state Zeeman sublevel (Fig. 7).

Moreover, the initially different populations of the sublevels are completely equalized at steady state, i.e., the sodium $D_1$ line is depolarized. This result is in accordance with what obtained in an earlier work [29], where no polarization of the D1 line fluorescence has been measured under excitation with a broadband linearly polarized light. This absence of atomic population accumulation to a certain Zeeman sublevel at $B=0$ is considered to be the reason for the MC resonance destruction at multimode excitation.

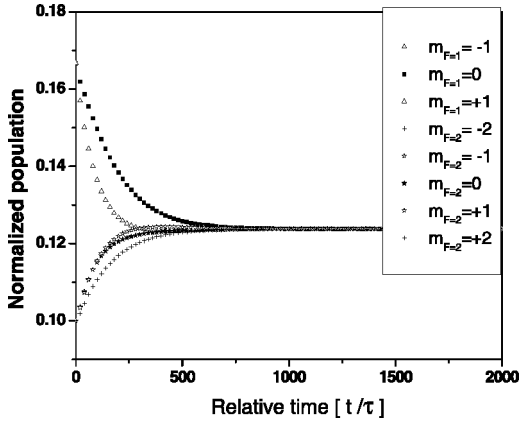


FIG. 7. Dynamics of the populations of the ground-state Zeeman sublevels for Na atoms under $\pi$ excitation (broadband spectrum; $I_L=400$ mW/cm$^2$).

Opposite to the $\pi$ excitation is the case of $\sigma^+$ excitation, where the light orients all atoms to states with maximum values of their angular momentum projection on the quantization axis (the laser light propagation direction). Our calculation has shown that if both ground-state levels are excited simultaneously, at steady state all atoms will be accumulated only on the ground-state sublevel $F_g=2$, $m_{F_g}=+2$ (Fig. 8).

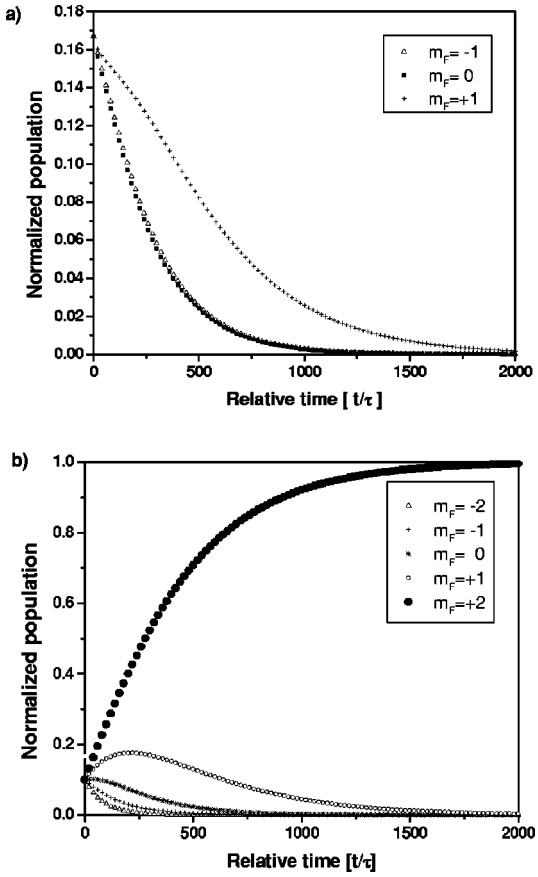


FIG. 8. Dynamics of the populations of the ground-state Zeeman sublevels of the hf levels (a) $F_g=1$ and (b) $F_g=2$, for Na atoms under broadband $\sigma^+$ excitation; $I_L=400$ mW/cm$^2$.

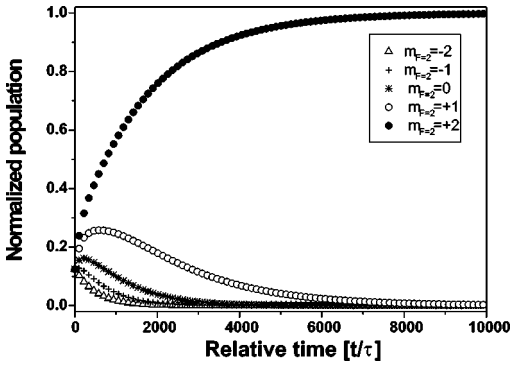


FIG. 9. Dynamics of the populations of the $F_g=2$ Zeeman sublevels under narrow band $\sigma^+$ excitation; $I_L=400$ mW/cm$^2$.

For narrow band excitation, it is shown in Fig. 9 that the time for the steady state establishment is significantly longer. This can be considered as a reason for lower MC resonance contrast observation at few-mode $\sigma^+$ excitation.

Consequently, exciting all hf transitions by broadband laser light, complete orientation of atoms along a single direction can be achieved. Due to the complete accumulation of atoms on a Zeeman sublevel not interacting with the laser field at B=0, the application of magnetic field $B_y$ will lead to a 100% contrast MC dark resonance. This is the case for coated and buffer gas cells, where the interaction time between atoms and light is large enough for reaching steady state. For the vacuum cell, the interaction time is less (about 10 $\mu$s) and hence there could still be some population left on the other Zeeman sublevels. Beside the dramatic increase of the MC resonance contrast, the complete orientation of atoms along a single direction is interesting for other purposes. In [30], using a single-frequency dye laser with 1 MHz jitter and a degree of circular polarization of 0.9998, by irradiating a Na beam, less than 50% atomic accumulation on the $F_g=2$, $m_{F_g}=+2$ level has been achieved. Under the conditions of the experiment presented in [11] even broadband pumping results in about 90% polarization of Rb. In our case 100% accumulation of atoms on a single level has been realized, which is evidenced by the observation of a 100% contrast MC resonance.

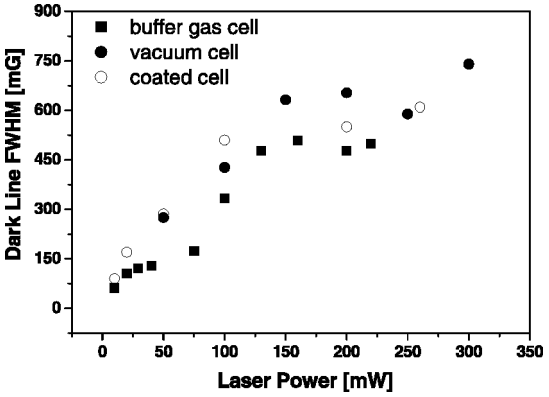


FIG. 10. MC resonance width as a function of the laser power. The cell temperature is 130 °C

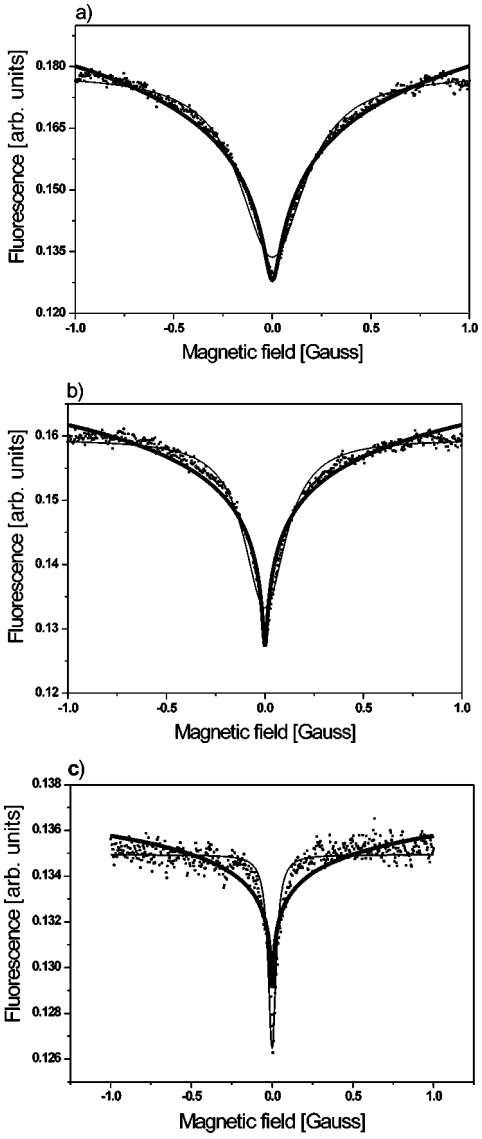


FIG. 11. Comparison of experimental and theoretical profiles of the MC resonances for buffer gas cell at 133 °C for three different laser power densities: (a) 360 mW/cm$^2$; (b) 270 mW/cm$^2$; (c) 36 mW/cm$^2$. The experimental profiles are presented by dots, the theoretical Lorentz profiles by solid lines and the profile calculated according to Eq. (7) by bold lines.

## V. FWHM AND PROFILE SHAPE OF THE MC RESONANCES

As expected, the influence of the radiation broadening on the MC resonance width in our experiment is less than the one observed in the case of single-frequency laser excitation having the same intensity. FWHM exceeding 1 G has been observed in Na for 0.1 W/cm$^2$ power density and single-frequency excitation [5]. In our experiments, the FWHM of the MC resonances remains below 1 G for laser power densities up to 1 W/cm$^2$.

The resonance width dependence on the power density is shown in Fig. 10 for the three Na cells under consideration. For a cell temperature of 130 °C, practically with the accuracy of our experiment there is no difference between the

resonance width observed in vacuum, coated and buffer gas cells. For lower temperature ($\sim$100 °C) the resonance width in the vacuum cell is two times larger than in the coated and buffer gas cells.

In principle, due to the increased interaction time of the atoms with the laser light, which is the case of buffer gas and coated cells, the FWHM is supposed to be about an order of magnitude less than in the vacuum cell. However, the Na density rising with temperature (for temperature change from 100 to 200 °C, the Na vapor pressure increases by three orders of magnitude) leads to a strong increment of the number of Na–Na collisions which can cause some relaxation of the Na atoms ground-state coherence and, hence, the broadening of the resonance. In contrast with the interactions responsible for the relaxation in buffer gases, the forces responsible for the spin exchange as a result of Na–Na collisions are of electrostatic nature and their cross-section is very large ($\sigma \approx 10^{-14}$ cm$^2$) [31].

In our experiment we also measure the influence of the laser power density on the shape of the MC resonances. This influence has been discussed in [32] for CPT resonances in Rb and Cs. There it has been shown that at low pumping rate the dark resonance has a Lorentzian shape with a FWHM given by

$$\Gamma^* = \gamma + \frac{\omega_R^2}{\Gamma}, \tag{6}$$

where $\omega_R$ is the Rabi frequency, $\gamma$ is the ground-state coherence relaxation rate and $\Gamma$ is the relaxation rate of the excited state. However, at high pumping rate, the resonance lineshape is quite different from a Lorentzian shape due to the effect of the Gaussian shape of the laser beam profile. In this case the resonance profile is given by the expression

$$f(\Omega) = \frac{1}{2} \ln \frac{\omega_R^2/\gamma\Gamma}{1 + (\Omega/\gamma)^2}. \tag{7}$$

Following this theoretical consideration, we compare the experimental MC resonance profiles with the theoretical ones for the buffer gas cell. The result is shown in Fig. 11.

It can be seen that in our case also the MC resonance has a Lorentzian shape only at very low pumping rate. Increasing the power density, the resonance profile differs significantly from the Lorentzian and it is in agreement with what is determined by Eq. (7). This can be considered a proof of the importance of the laser beam profile

## VI. CONCLUSIONS

Strong enhancement of the contrast of the MC resonances in Na vapor up to 100% has been achieved by increasing the spectral interval of the laser field with $\sigma^+$ excitation. For laser power density from 0.1 to 1 W/cm$^2$, the FWHM of the resonance ranges in an interval of 90-400 kHz. This complete transparency of the medium in a narrow spectral interval is interesting for the purposes of the enhancement of its refractive index and of the signal-to-noise ratio of the dark resonances. The signal-to-noise ratio enhancement is very important for application of such resonances in precise measurements of weak magnetic fields. For excitation by linearly polarized light, the MC resonance vanishes when the number of modes of the laser is increased. This behavior is supported by theoretical calculation of the atomic population distribution among the Zeeman sublevels of the two ground-state hf levels for two laser polarizations and without consideration of the coherence induced by the optical fields. This complete orientation of atoms is evidenced experimentally by the observation of 100% transparency of the medium.

## ACKNOWLEDGMENTS

This work was done under a collaboration program between the National Research Council of Italy and the Bulgarian Academy of Sciences. The authors would like to thank M. Badalassi and M. Tagliaferri for the technical assistance, Professor A. Weis for the very helpful discussions on the experimental results. S.C. and T.K. acknowledge the Bulgarian NCSR for the support (Grant No. F1005/00). We are grateful to the EC for the partial support of this investigation (Contract No. G6RD-CT-2001-00642).

[1] A. Aspect, E. Arimondo, R. Kaiser, N. Vansteenkiste, and C. Cohen-Tannoudji, Phys. Rev. Lett. **61**, 826 (1988).

[2] A. Nagel, L. Graf, A. Naumov, E. Mariotti, V. Biancalana, D. Meschede, and R. Wynands, Europhys. Lett. **44**, 31 (1998); R. Wynands and A. Nagel, Appl. Phys. B: Lasers Opt. **B68**, 1 (1999).

[3] M. Zhu and L. S. Cutler, US Patent No. 6,201,821 B1, March 13, 2001, *Coherent population trapping-based frequency standard having a reduced magnitude of total a.c. stark shift*; J. Kitching, L. Hollberg, S. Knappe, R. Wynands, Electron. Lett. **37**, 1449 (2001).

[4] L. V. Hau, S. E. Harris, Z. Dutton, and C. H. Behroozi, Nature (London) **397**, 594 (1999).

[5] F. Renzoni, W. Maichen, L. Windholz, and E. Arimondo, Phys. Rev. A **55**, 3710 (1997).

[6] G. Alzetta, A. Gozzini, L. Moi, and G. Orriols, Nuovo Cimento Soc. Ital. Fis., B **36B**, 5 (1976); G. Alzetta, L. Moi, and G. Orriols, *ibid.* **52**, 209 (1979); J. H. Xu, G. Alzetta, Phys. Lett. A **248**, 80 (1998); S. Gozzini, P. Sartini, G. Gabbanini, A. Lucchesini, C. Marinelli, L. Moi, J. H. Xu, and G. Alzetta, Eur. Phys. J. D **6**, 127 (1999).

[7] K. Motomura and M. Mitsunaga, J. Opt. Soc. Am. B **19**, 2456 (2002).

[8] A. S. Zibrov, M. D. Lukin, L. Hollberg, D. E. Nikonov, M. O. Scully, H. C. Robinson, and V. L. Velichansky, Phys. Rev. Lett. **76**, 3935 (1996).

[9] O. Kocharovskaya, Y. Rostovtsev, and M. O. Scully, Phys. Rev. Lett. **86**, 628 (2001); D. F. Phillips, A. Fleischhauer, A.

Mair, R. L. Walsworth, and M. D. Lukin, *ibid.* **86**, 783 (2001).
[10] W. Happer, Rev. Mod. Phys. **44**, 169 (1972).
[11] E. Babcock, I. Nelson, S. Kadlecek, B. Driehuys, L. W. Anderson, F. W. Hersman, and T. G. Walker, Phys. Rev. Lett. **91**, 123003 (2003).
[12] L. Moi, Opt. Commun. **50**, 349 (1984).
[13] S. Gozzini, E. Mariotti, C. Gabbanini, A. Lucchesini, C. Marinelli, and L. Moi, Appl. Phys. B: Photophys. Laser Chem. **B54**, 428 (1992).
[14] D. Budker, W. Gawlik, D. F. Kimball, S. M. Rochester, V. V. Yashchuk, and A. Weis, Rev. Mod. Phys. **74**, 1153 (2002).
[15] M. Graf, E. Arimondo, E. S. Fry, D. E. Nikonov, G. G. Padmabandu, M. O. Scully, and S.-Y. Zhu, Phys. Rev. A **51**, 4030 (1995); D. A. Steck, http://george.ph.utexas.edu/~dsteck/alkalidata/.
[16] F. Renzoni, C. Zimmermann, P. Verkerk, and E. Arimondo, J. Opt. B: Quantum Semiclassical Opt. **1**, S7 (2001).
[17] A. V. Taichenachev, A. M. Tumaikin, and V. I. Yudin, JETP Lett. **69**, 819 (1999).
[18] A. V. Taichenachev, A. M. Tumaikin, V. I. Yudin, Phys. Rev. A **61**, 011802(R) (2000).
[19] A. V. Papoyan, A. Auzinsh, and K. Bergmann, Eur. Phys. J. D **21**, 63 (2002).
[20] J. Alnis and A. Auzinsh, J. Phys. B **34**, 3889 (2001).
[21] F. Renzoni and E. Arimondo, Europhys. Lett. **46**, 716 (1999).
[22] C. Andreeva, S. Cartaleva, Y. Dancheva, V. Biancalana, A. Burchianti, C. Marinelli, E. Mariotti, L. Moi, and K. Nasyrov, Phys. Rev. A **66**, 012502 (2002).
[23] S. Knappe, J. Kitching, L. Hollberg, R. Wynands, Appl. Phys. B: Lasers Opt. **B74**, 217 (2002).
[24] G. Ankerhold, M. Schiffer, D. Mutschall, T. Scholz, W. Lange, Phys. Rev. A **48**, R4031 (1993).
[25] S. Gozzini, P. Sartini, C. Gabbanini, A. Lucchesini, L. Moi, C. Marinelli, G. Alzetta, and J. H. Xu, Opt. Commun. **160**, 75 (1999).
[26] Y. Nafcha, M. Rosenbluh, P. Tremblay, and C. Jacques, Phys. Rev. A **52**, 3216 (1995).
[27] Y. Nafcha, D. Albeck, and M. Rosenbluh, Phys. Rev. Lett. **67**, 2279 (1991).
[28] C. Cohen-Tannoudji, in *Frontiers in Laser Spectroscopy*, Les Houches Lectures, edited by R. Balian, S. Haroche, and S. Liberman (North-Holland, Amsterdam, 1975), Vol. I, p. 1.
[29] A. C. G. Mitchel and M. W. Zemansky, *Resonance Radiation and Excited Atoms* (Cambridge U. P., London, 1934).
[30] J. J. McClelland and M. H. Kelley, Phys. Rev. A **31**, 3704 (1985).
[31] A. Corney, *Atomic and Laser Spectroscopy* (Clarendon, Oxford, 1977).
[32] F. Levi, A. Godone, J. Vanier, S. Micalizio, and G. Modugno, Eur. Phys. J. D **12**, 53 (2000).